

New Results on Hyperons from NA48/1

Matthias Behler*

Johannes Gutenberg-Universität, 55099 Mainz, Germany

October 31, 2006

Abstract

Several new results from the NA48/1 collaboration on hyperon decays are presented: the Ξ^0 lifetime was measured with very high accuracy using about 130,000 $\Xi^0 \rightarrow \Lambda\pi^0$ decays; large samples of the weak radiative decays $\Xi^0 \rightarrow \Lambda\gamma$ and $\Xi^0 \rightarrow \Sigma^0\gamma$ as well as of the semileptonic decay $\Xi^0 \rightarrow \Sigma^+e^-\bar{\nu}_e$ were collected, leading to asymmetry and BR measurements much more precise than results from previous experiments. The muon mode of the semileptonic decay, $\Xi^0 \rightarrow \Sigma^+\mu^-\bar{\nu}_\mu$, was observed with 99 candidates. From the $\Xi^0 \rightarrow \Sigma^+e^-\bar{\nu}_e$ branching ratio the CKM matrix element $|V_{us}|$ was extracted.

1 Introduction

After more than 50 years of both theoretical and experimental investigations, many properties of hyperons are still barely understood [1]. On the theoretical side, the complexity of calculations involving the strong interactions is usually the reason invoked. The limited theoretical understanding becomes particularly apparent when comparing, e.g., predictions and measured values for baryon magnetic moments, polarization of hyperons produced in nucleon-nucleon-collisions, or decay asymmetries of weak radiative decays. Even more, some experimental results, like the polarization of the anti-hyperons $\bar{\Xi}^+$ and $\bar{\Sigma}^-$ produced in nucleon-nucleon-collisions (while other anti-hyperons are non-polarized), cannot be explained at all by any of the existing models.

On the experimental side, most of the hadronic hyperon decays are fairly well measured while for most of their radiative or semileptonic decays only a few hundred events are collected. Now, the experimental situation has improved thanks to the recent high intensity kaon experiments, like NA48/1, which collected large data samples of neutral hyperons.

*On behalf of the NA48/1 collaboration: Cambridge – CERN – Chicago – Dubna – Edinburgh – Ferrara – Firenze – Mainz – Northwestern – Perugia – Pisa – Saclay – Siegen – Torino – Wien.

2 The Experimental Setup

The NA48 experiment at the CERN SPS was originally built to measure the parameter $\Re(\varepsilon'/\varepsilon)$ of direct CP violation in the neutral kaon decays $K^0 \rightarrow 2\pi$ [2]. In the second phase of the experiment, called NA48/1, the main goal was the study of neutral hyperon and rare K_S decays. The data were taken mainly in 2002 with some small test runs in 1999 and 2001 as well as in a period in 2000 without drift chambers, since they were damaged in 1999.

A beam of neutral long-lived particles (K^0 , Λ , Ξ^0 , n , γ) was produced by a 400 GeV/c proton beam impinging on a Beryllium target. The intensity of the proton beam was about 200 times larger than in the ε'/ε runs, with a mean of $5 \cdot 10^{10}$ protons per pulse. A production angle of 4.8 mrad was chosen to reduce the number of neutrons in the neutral beam, leading to a transverse polarization of the hyperons of about -10%. The charged particles were deflected by a sweeping magnet immediately after the target. The last collimator 6 m after the target was followed by a 90 m long evacuated tank containing the fiducial decay region. The detector was located downstream of this tank.

The main components of the detector were the magnetic spectrometer and the electromagnetic calorimeter. The spectrometer consisted of two drift chambers before and two after a dipole magnet to measure the momentum of charged particles with a resolution of $\sigma_p/p = 0.48\% \oplus 0.015\% \cdot p$, where p is in GeV/c. The time measurement for charged particles was performed by a hodoscope of fast scintillators with a resolution of about 250 ps.

Neutral particles were detected by the liquid krypton electromagnetic calorimeter (LKr) with an active volume of almost 7 m³, divided into ~ 13300 cells with a size of $2 \times 2 \times 125$ cm³ corresponding to a thickness of 27 radiation lengths. The energy resolution of the calorimeter was $\sigma_E/E = 3.2\%/\sqrt{E} \oplus 9.0\%/E \oplus 0.42\%$, where E is in GeV.

An iron-scintillator sandwich hadron calorimeter and muon counters were located further downstream. The experimental layout is described in detail elsewhere [3].

3 Hyperon Physics in NA48/1

The 89 days of data taking in 2002 led to a total flux in the fiducial region of $3.5 \cdot 10^{10}$ K_S and $2.4 \cdot 10^9$ Ξ^0 decays. About 3 million fully reconstructed events of the main decay mode $\Xi^0 \rightarrow \Lambda\pi^0$ have been collected. Besides being used as normalization for branching ratio measurements, they also

allow the determination of the Ξ^0 mass, lifetime, and production polarization. Several 10^4 events of the weak radiative decays $\Xi^0 \rightarrow \Lambda\gamma$ and $\Xi^0 \rightarrow \Sigma^0\gamma$ were reconstructed, whose decay asymmetries are of particular interest to test contradictory theoretical predictions. For the semileptonic decays $\Xi^0 \rightarrow \Sigma^+e^-\bar{\nu}_e$ and $\Xi^0 \rightarrow \Sigma^+\mu^-\bar{\nu}_\mu$ about $6 \cdot 10^3$ and 99 reconstructed events were collected, respectively. The measurement of their branching ratios allows the determination of the CKM matrix element $|V_{us}|$. The NA48/1 experiment was also searching for rare Ξ^0 decays like $\Xi^0 \rightarrow \Lambda e^+e^-$ or $\Xi^0 \rightarrow p\pi^-$ ($\Delta S = 2$), the former being observed for the first time.

The new measurements of the Ξ^0 lifetime (Sec. 4), the decay asymmetries of the radiative decays (Sec. 5) and the branching ratios of the semileptonic decays (Sec. 6) performed with the 2002 data are presented here.

4 Ξ^0 Lifetime

The Ξ^0 lifetime is an important input to other measurements, first of all to the determination of $|V_{us}|$ via the decay rate of the semileptonic Ξ^0 decays (Eq. 9), but also to the simulation needed for all measurements. Its current precision is only about 3%, measured by experiments that took place in the 60's and 70's [4].

Using a minimum bias trigger, about 260,000 $\Xi^0 \rightarrow \Lambda\pi^0$ decays have been selected with negligible background. The minimum bias trigger has the advantage of a very high efficiency of $(99.56 \pm 0.02)\%$, but was downscaled during the data taking. A full Monte Carlo simulation was performed using the current mean Ξ^0 lifetime [4] and compared to the data in 10 bins of the Ξ^0

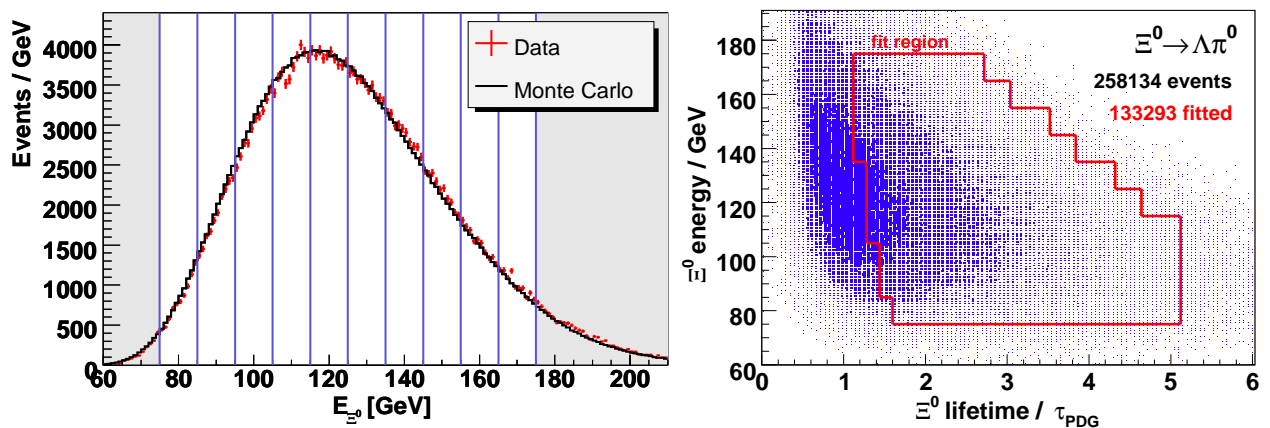


Figure 1: Ξ^0 energy distribution for selected $\Xi^0 \rightarrow \Lambda\pi^0$ minimum bias events with the 10 energy bins used for the lifetime fit (left), and Ξ^0 energy distribution versus proper lifetime for the same events (right). The fit region is indicated by the red enclosure.

energy, to avoid a bias from the energy spectrum used in the simulation. The ratios of the lifetime distributions were simultaneously fitted with 10 normalizations and the Ξ^0 lifetime as free parameters. The fit regions started about one lifetime downstream of the collimator in order to avoid detector resolution effects. This reduced the number of events used in the fit to about 130,000. The energy distribution for the selected events and the fit region in energy and lifetime are shown in Fig. 1.

From the fit, the ratio $\frac{\tau_{data}}{\tau_{PDG}} = 1.0626 \pm 0.0044_{stat} \pm 0.0043_{syst}$ was obtained as a preliminary result, corresponding to

$$\tau_{\Xi^0} = (3.082 \pm 0.013_{stat} \pm 0.012_{syst}) \cdot 10^{-10} \text{ s}. \quad (1)$$

The agreement between data and fitted MC is very good (Fig. 2). As a systematic check, the energy bins were also fitted independently and the obtained results are consistent with the combined fit. All sources of systematic uncertainty are summarized in Tab. 3. The main contributions come from the detector acceptance and the calorimeter energy scale. The result is about two standard deviations above the current PDG average and five times more precise (Fig. 3).

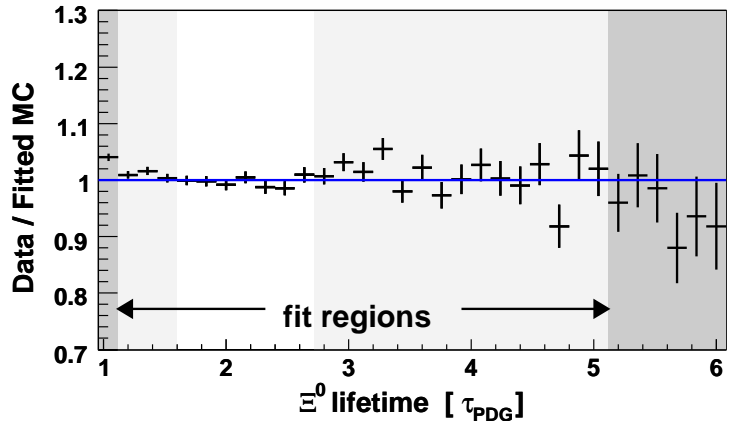


Figure 2: Data divided by fitted MC. In the light grey region not all energy bins were included in the fit, the dark grey region was excluded.

Source	$\Delta_{syst}/\tau_{PDG}(\%)$
Detector acceptance	± 0.30
Vertex resolution	± 0.08
Energy scale	± 0.14
Energy non-linearities	± 0.09
Ξ^0 polarization	± 0.15
Ξ^0 mass	± 0.20
Λ lifetime	± 0.04
Total systematics	± 0.43
Statistical uncertainty	± 0.44

Table 1: Systematic uncertainties of the Ξ^0 lifetime measurement.

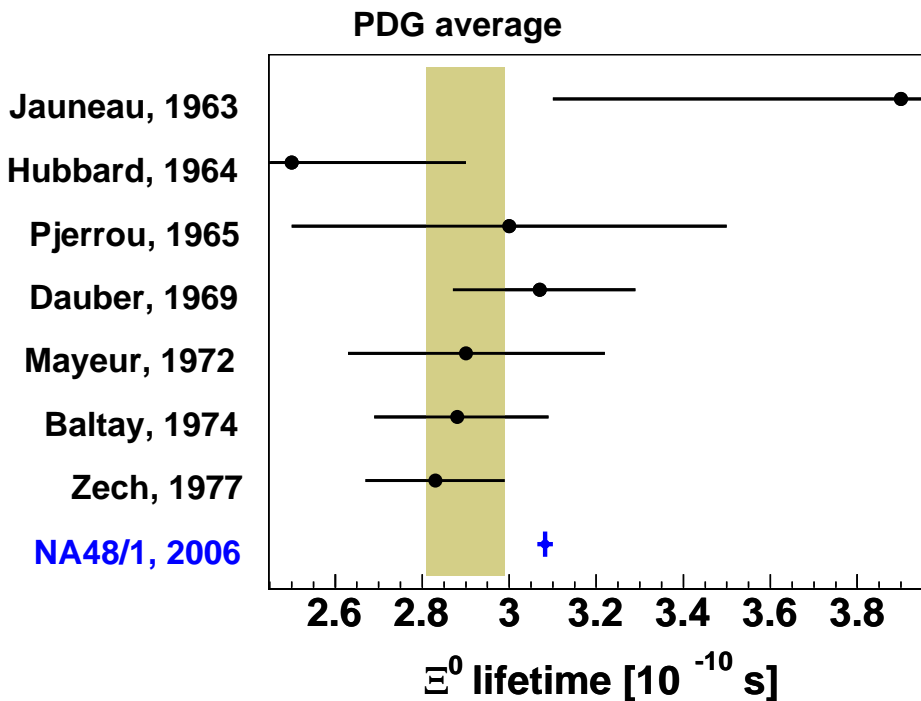


Figure 3: Comparison between the new NA48/1 result and the previous measurements. The yellow band indicates the PDG average and its uncertainty.

5 Ξ^0 Decay Asymmetries

Up to this day, weak radiative hyperon decays, such as $\Xi^0 \rightarrow \Lambda \gamma$ or $\Xi^0 \rightarrow \Sigma^0 \gamma$ are still not understood. Several competing theoretical models give very different predictions. An excellent experimental parameter to distinguish between models is the decay asymmetry α . It is defined as

$$\frac{dN}{d \cos \Theta} = N_0(1 + \alpha |\vec{P}| \cos \Theta), \quad (2)$$

where Θ is the angle between the direction of the daughter baryon and the polarization \vec{P} of the mother in the mother's rest frame.

Since the Ξ^0 polarisation is not precisely known, the asymmetry of the decay $\Lambda \rightarrow p \pi^-$ is used instead. For example, in the decay $\Xi^0 \rightarrow \Lambda \gamma$ the asymmetry $\alpha_{\Xi^0 \rightarrow \Lambda \gamma}$ can be measured by looking at the angle Θ_Λ between the incoming Ξ^0 and the outgoing proton from the subsequent $\Lambda \rightarrow p \pi^-$ decays in the Λ rest frame (Fig. 4). The angular distribution for Θ_Λ is given by

$$\frac{dN}{d \cos \Theta_\Lambda} = N_0(1 - \alpha_{\Xi^0 \rightarrow \Lambda \gamma} \alpha_{\Lambda \rightarrow p \pi^-} \cos \Theta_\Lambda), \quad (3)$$

where $\alpha_{\Lambda \rightarrow p \pi^-}$ is the asymmetry of the Λ decay. Using this method, the measurement is independent of the initial Ξ^0 polarization.

In case of the $\Xi^0 \rightarrow \Sigma^0 \gamma$, the subsequent decay $\Sigma^0 \rightarrow \Lambda \gamma$ has to be taken into account. Defining two angles similar to Fig. 4, $\Theta_{\Xi^0 \Lambda}$ between the incoming Ξ^0 and the outgoing Λ in the Σ^0 rest frame and $\Theta_{\Sigma^0 p}$ between the incoming Σ^0 and the outgoing proton in the Λ rest frame, the full decay chain is described by a two-dimensional angular distribution

$$\frac{d^2 N}{d \cos \Theta_{\Xi \Lambda} d \cos \Theta_{\Sigma p}} = N_0 (1 + \alpha_{\Xi^0 \rightarrow \Sigma^0 \gamma} \alpha_{\Lambda \rightarrow p \pi^-} \cos \Theta_{\Xi \Lambda} \cos \Theta_{\Sigma p}). \quad (4)$$

From the 2002 data, 48,314 $\Xi^0 \rightarrow \Lambda \gamma$ and 13,068 $\Xi^0 \rightarrow \Sigma^0 \gamma$ candidates were selected (Fig. 5). The background contaminations were 0.8% for $\Xi^0 \rightarrow \Lambda \gamma$ and about 3% for $\Xi^0 \rightarrow \Sigma^0 \gamma$, respectively. The angular distributions defined above were compared to full Monte Carlo simulations with no Ξ^0 asymmetry. For the decay $\Xi^0 \rightarrow \Sigma^0 \gamma$, the product $\cos \Theta_{\Xi \Lambda} \cos \Theta_{\Sigma p}$ was used to perform a one-dimensional fit. Both fits show the expected linear behaviour on the angular parameters, and the slopes were measured to be $\alpha_{\Xi^0 \rightarrow \Lambda \gamma} \alpha_{\Lambda \rightarrow p \pi^-} = -0.439 \pm 0.013_{stat} \pm 0.038_{syst}$ and $\alpha_{\Xi^0 \rightarrow \Sigma^0 \gamma} \alpha_{\Lambda \rightarrow p \pi^-} = -0.438 \pm 0.020_{stat} \pm 0.041_{syst}$, respectively. Unfolding the well-known asymmetry $\alpha_{\Lambda \rightarrow p \pi^-} = 0.642 \pm 0.013$ [4], we obtained the preliminary results

$$\alpha_{\Xi^0 \rightarrow \Lambda \gamma} = -0.684 \pm 0.020_{stat} \pm 0.061_{syst}, \quad (5)$$

$$\alpha_{\Xi^0 \rightarrow \Sigma^0 \gamma} = -0.682 \pm 0.031_{stat} \pm 0.065_{syst}. \quad (6)$$

Several systematic checks were performed (Tab. 2), in particular by testing the measurement of the well-known $\Xi^0 \rightarrow \Lambda \pi^0$ decays asymmetry. About $3 \cdot 10^6$ candidates of this decay were reconstructed with negligible background. The same method as for $\Xi^0 \rightarrow \Lambda \gamma$ was used and gave the result $\alpha_{\Xi^0 \rightarrow \Lambda \pi^0} = -0.439 \pm 0.004_{stat} \pm 0.045_{syst}$, in very good agreement with the PDG average of -0.411 ± 0.022 [4].

The obtained values agree with previous measurements by NA48 on $\Xi^0 \rightarrow \Lambda \gamma$ ($\alpha_{\Xi^0 \rightarrow \Lambda \gamma} = -0.78 \pm 0.19$ [5]) and KTeV on $\Xi^0 \rightarrow \Sigma^0 \gamma$ ($\alpha_{\Xi^0 \rightarrow \Sigma^0 \gamma} = -0.63 \pm 0.09$ [6]), but are much more precise. In particular the result on $\Xi^0 \rightarrow \Lambda \gamma$ is of high theoretical interest, as it confirms the large negative value of the

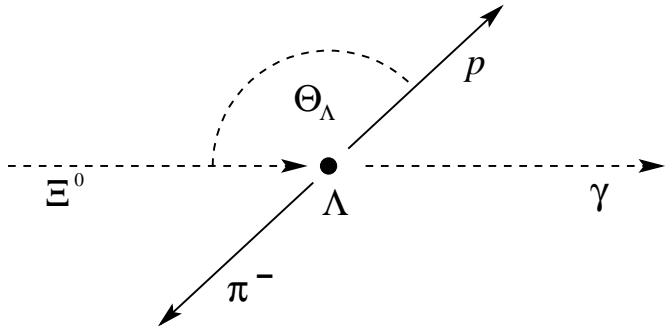


Figure 4: Definition of the angle Θ_{Λ} between the proton and the incoming Ξ^0 in the Λ rest frame.

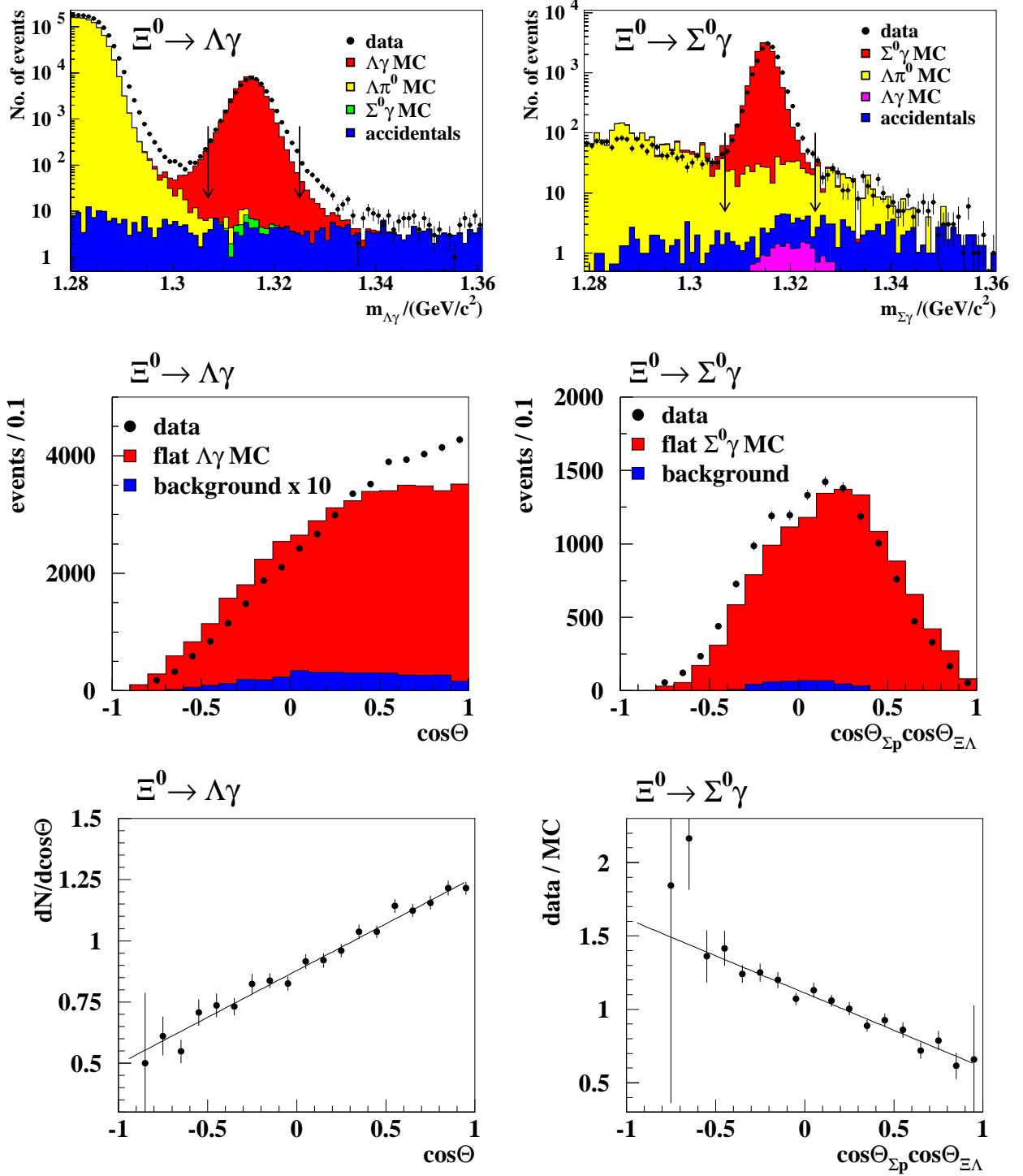


Figure 5: Invariant mass distributions (top), angular distributions (middle) and fits of the decay asymmetries (bottom) for $\Xi^0 \rightarrow \Lambda \gamma$ (left) and $\Xi^0 \rightarrow \Sigma^0 \gamma$ (right). In the top and middle plots, the MC expectation for signal and background is compared to the data.

decay asymmetry, which is difficult to accommodate for quark and vector meson dominance models.

	$\Delta(\alpha_{\Xi}\alpha_{\Lambda})$		
	$\Xi \rightarrow \Lambda\gamma$	$\Xi \rightarrow \Sigma^0\gamma$	$\Xi \rightarrow \Lambda\pi^0$
Trigger efficiency	0.016	0.024	0.001
Ξ^0 polarization	—	—	0.002
Detector geometry / selection	0.021	0.021	0.012
Ξ^0 energy dependence	0.025	0.025	0.025
Ξ^0 mass	0.011	0.004	0.005
Ξ^0 lifetime	0.001	0.007	0.003
$\Lambda\pi^0$ background	0.001	—	—
Total systematics	0.038	0.041	0.028
Statistical error (data+MC)	0.013	0.020	0.003

Table 2: Total systematic uncertainties of the asymmetry measurements.

6 Semileptonic Ξ^0 Decays and $|V_{us}|$

From the theoretical point of view, the semileptonic Ξ^0 decays ($\Xi^0 \rightarrow \Sigma^+ e^- \bar{\nu}_e$ and $\Xi^0 \rightarrow \Sigma^+ \mu^- \bar{\nu}_\mu$) are interesting essentially for two reasons: they allow the determination of the CKM matrix element $|V_{us}|$ via the measurement of their branching ratios, while the study of the form factors appearing in the decay amplitudes is a useful tool to search for $SU(3)_f$ breaking effects. In exact $SU(3)_f$, the form factors from the Ξ^0 and the neutron β decays are identical.

Due to the presence of the neutrino, a full reconstruction of the Ξ^0 decays is not possible. Since NA48/1 used a neutral beam and the two-body decay $\Xi^0 \rightarrow \Sigma^+ \pi^-$ is kinematically forbidden, the semileptonic Ξ^0 decays are the only source of Σ^+ 's. This allows to identify these decays by the reconstruction of the subsequent decay $\Sigma^+ \rightarrow p\pi^0$ together with an associated positively identified lepton. With this method 6,238 $\Xi^0 \rightarrow \Sigma^+ e^- \bar{\nu}_e$ and 99 $\Xi^0 \rightarrow \Sigma^+ \mu^- \bar{\nu}_\mu$ candidates were reconstructed (Fig. 6). The background estimated from the mass side-bands was 2.4% for the electron mode and about 31% for the muon mode, respectively.

The normalizations used to calculate the branching ratios were $\Xi^0 \rightarrow \Lambda\pi^0$ decays in the case of the electron mode and the muon mode in case of the muon mode. The preliminary results we obtained are

$$BR_{\Xi^0 \rightarrow \Sigma^+ e^- \bar{\nu}_e} = (2.51 \pm 0.03_{stat} \pm 0.11_{syst}) \cdot 10^{-4}, \quad (7)$$

$$BR_{\Xi^0 \rightarrow \Sigma^+ \mu^- \bar{\nu}_\mu} = (2.2 \pm 0.3_{stat} \pm 0.2_{syst}) \cdot 10^{-6}. \quad (8)$$

The largest contribution to the systematic uncertainty for the $\Xi^0 \rightarrow \Sigma^+ e^- \bar{\nu}_e$ branching ratio is the uncertainty on the acceptance due to the badly known form factors and polarization which were used in the simulation. In the case of the muon mode the systematic uncertainty is dominated by the background estimate, trigger efficiency and the uncertainty on the branching ratio of the normalization channel. Both results are compatible with previous measurements by KTeV ($BR_{\Xi^0 \rightarrow \Sigma^+ e^- \bar{\nu}_e} = (2.7 \pm 0.4) \cdot 10^{-4}$ [7] and $BR_{\Xi^0 \rightarrow \Sigma^+ \mu^- \bar{\nu}_\mu} = (4.9_{-1.6}^{+2.1}) \cdot 10^{-6}$ [8]), but have much smaller uncertainties.

The theoretical calculation using $SU(3)_f$ symmetry predicts $BR_{\Xi^0 \rightarrow \Sigma^+ e^- \bar{\nu}_e} = 2.6 \cdot 10^{-4}$ [9]. Taking into account only the different phase space one would expect $BR_{\Xi^0 \rightarrow \Sigma^+ e^- \bar{\nu}_e} = 114 \times BR_{\Xi^0 \rightarrow \Sigma^+ \mu^- \bar{\nu}_\mu}$. Since both predictions are in very good agreement with the presented measurements no hint for large $SU(3)_f$ breaking effects or violation of lepton universality are found.

The parameter $|V_{us}|$ can be extracted from the measured Ξ^0 decay rate using [10]

$$\begin{aligned} \Gamma &= \frac{BR_{\Xi^0 \rightarrow \Sigma^+ e^- \bar{\nu}_e}}{\tau_{\Xi^0}} \\ &= G_f^2 V_{us}^2 \frac{\Delta m^5}{60 \pi^3} (1 + \delta_{rad}^{MD})(1 + \delta_{rad}^{MI}) \left\{ \left(1 - \frac{3}{2}\beta\right) (|f_1^2| + 3|g_1^2|) \right. \\ &\quad \left. + \frac{6}{7}\beta^2 (|f_1^2| + 2|g_1^2| + \Re(f_1 f_2^*) + \frac{2}{3}|f_2^2|) + \delta_{q^2}(f_1, g_1) \right\}, \end{aligned} \quad (9)$$

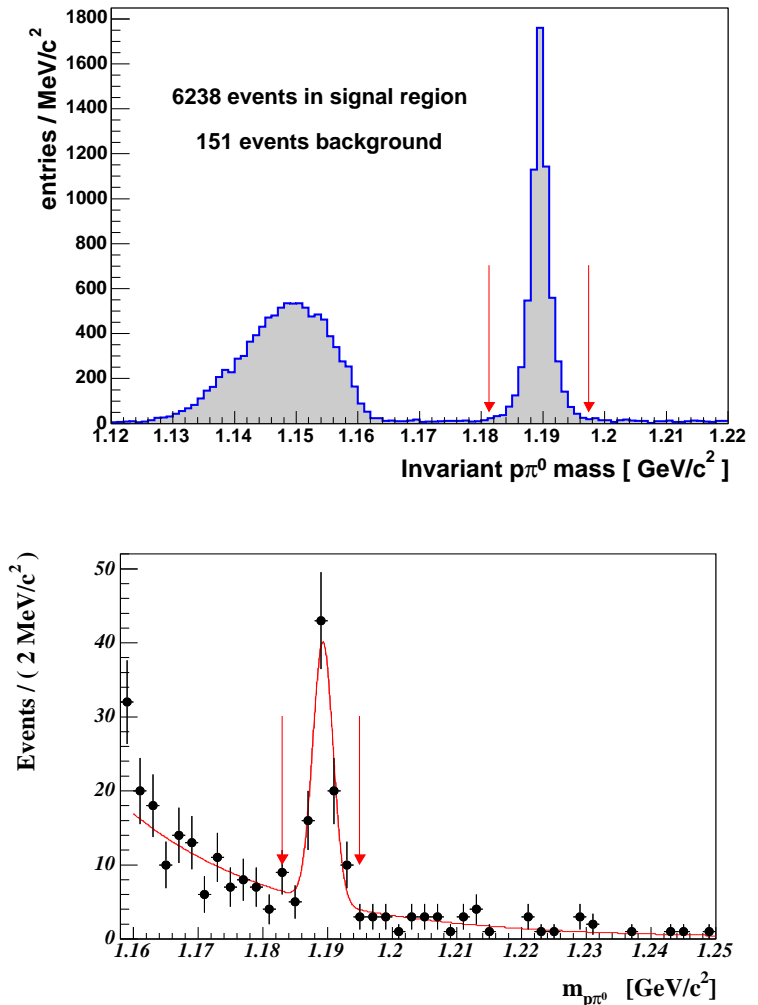


Figure 6: Distribution of the invariant proton π^0 mass with an associated positively identified electron (top) and with an associated positively identified muon (bottom).

where $\tau_{\Xi^0} = (2.90 \pm 0.09) \cdot 10^{-10}$ s is the Ξ^0 lifetime, $\Delta m = m_{\Xi^0} - m_{\Sigma^+} = (0.12546 \pm 0.00021)$ GeV/ c^2 and $\beta = \frac{\Delta m}{m_{\Xi^0}} = 0.09542 \pm 0.00011$ [4]. $\delta_{rad}^{MD} = 0.0211$ and $\delta_{rad}^{MI} = 0.0226$ are the model dependent and model independent radiative corrections, respectively. $\delta_{q^2}(f_1, g_1) = 0.119$ takes into account the dependence of the form factors f_1 and g_1 on the transferred momentum [10]. Using the current experimental values for g_1/f_1 and f_2/f_1 [11], $|V_{us}|$ was found to be

$$|V_{us}| = 0.214 \pm 0.006_{exp} \begin{matrix} +0.030 \\ -0.025_{syst} \end{matrix}. \quad (10)$$

The uncertainty is dominated by the experimental precision on g_1/f_1 . The obtained value is consistent with the measurements from kaon decays ($|V_{us}| = 0.2257 \pm 0.0021$ [4]) and from various hyperon semileptonic decays ($|V_{us}| = 0.2250 \pm 0.0027$ [12]).

References

- [1] See, e.g., D. Chang, hep-ph/0011163, Nov 2000; and references therein.
- [2] J.R. Batley et al., Phys. Lett. **B 544** (2002) 97.
- [3] A. Lai et al., Eur. Phys. J. **C 22** (2001) 231.
- [4] W.-M. Yao et al., J. Phys. **G 33** (2006).
- [5] A. Lai et al., Phys. Lett. **B 584** (2004) 251.
- [6] A. Alavi-Harati et al., Phys. Rev. Lett. **86**, (2001) 3239.
- [7] A. Affolder et al., Phys. Rev. Lett. **82**, (1999) 3751.
- [8] E. Abouzaid et al., Phys. Rev. Lett. **95**, (2005) 81801.
- [9] N. Cabibbo, Phys. Rev. Lett. **10** (1963) 531.
- [10] A. Garcia, P. Kielanowski, Lecture Notes in Physics Vol. 222 (Springer-Verlag, Berlin, 1985).
- [11] A. Alavi-Harati et al., Phys. Rev. Lett. **87** (2001) 132001.
- [12] N. Cabibbo, E.C. Swallow and R. Winston, Phys. Rev. Lett. **92** (2004) 251803.